Jian Li and Petre Stoica

MIMO Radar with Colocated Antennas

Review of some recent work

A multi-input multi-output (MIMO) radar system, unlike standard phased-array radar, can transmit, via its antennas, multiple probing signals that may be correlated or uncorrelated with each other. While the companion article by Blum et al., to appear in the November issue, exploited the diversity offered by widely separated transmit/receive antenna elements, we focus on the merits of the waveform diversity allowed by transmit and receive antenna arrays containing elements that are colocated. For the latter type of MIMO radar systems, we provide an overview of recent results showing that the waveform diversity enables the MIMO radar superiority in several fundamental aspects, including: 1) significantly improved parameter identifiability, 2) direct applicability of adaptive arrays for target detection and parameter estimation, and 3) much enhanced flexibility for transmit beampattern design. Specifically, we show that 1) the maximum number of targets that can be uniquely identified by the MIMO radar is up to M_t times that of its phased-array counterpart, where M_t is the number of transmit antennas, 2) the echoes due to targets at different locations can be linearly independent of each other, which allows the

Digital Object Identifier 10.1109/MSP.2007.904812

1053-5888/07/$25.00©2007IEEE

direct application of many adaptive techniques to achieve high resolution and excellent interference rejection capability, and 3) the probing signals transmitted via its antennas can be optimized to obtain several transmit beampattern designs with superior performance. For example, the covariance matrix of the probing signal vector transmitted by the MIMO radar can be optimized to maximize the power around the locations of the targets of interest and also to minimize the cross-correlation of the signals reflected back to the radar by these targets, thereby significantly improving the performance of adaptive MIMO radar techniques. Additionally, we demonstrate the advantages of several MIMO transmit beampattern designs, including a beampattern matching design and a minimum sidelobe beampattern design, over their phased-array counterparts. In conclusion, the two articles in this issue show that MIMO radar is a fertile research ground that merits further investigation, including reaping the full benefits of both types of diversity covered in the two articles.

INTRODUCTION

MIMO radar is an emerging technology that is attracting the attention of researchers and practitioners alike. Unlike a standard phased-array radar, which transmits scaled versions of a single waveform, a MIMO radar system can transmit via its antennas multiple probing signals that may be chosen quite freely (see Figure 1). This waveform diversity enables superior capabilities compared with a standard phased-array radar. In [1]–[3], for example, the diversity offered by widely separated transmit/receive antenna elements is exploited. Many other papers, including, for instance, [4]–[21], have considered the merits of a MIMO radar system with colocated antennas. For colocated transmit and receive antennas, the MIMO radar paradigm has been shown to offer higher resolution (see, e.g., [4], [5]), higher sensitivity to detecting slowly moving targets [6], better parameter identifiability [11], [19], and direct applicability of adaptive array techniques [11], [13]. Waveform optimization has also been shown to be a unique capability of a MIMO radar system. For example, it has been used to achieve flexible transmit beampattern designs (see, e.g., [7], [15]–[17]) as well as for MIMO radar imaging and parameter estimation [10], [20], [21].

We provide herein an overview of our recent results showing that this waveform diversity enables the MIMO radar superiority in several fundamental aspects. Without loss of generality, we consider targets associated with a particular range and Doppler bin. Targets in adjacent range bins contribute as interferences to the range bin of interest.

First we address a basic aspect on MIMO radar—its parameter identifiability, which is the maximum number of targets that can be uniquely identified by the radar. We show that the waveform diversity afforded by MIMO radar enables a much improved parameter identifiability over its phased-array counterpart, i.e., the maximum number of targets that can be uniquely identified by the MIMO radar is up to M_t times that of its phased-array counterpart, where M_t is the number of transmit antennas. The parameter identifiability is further demonstrated in a numerical study using both the Cramér-Rao bound (CRB) and a least-squares method for target parameter estimation.

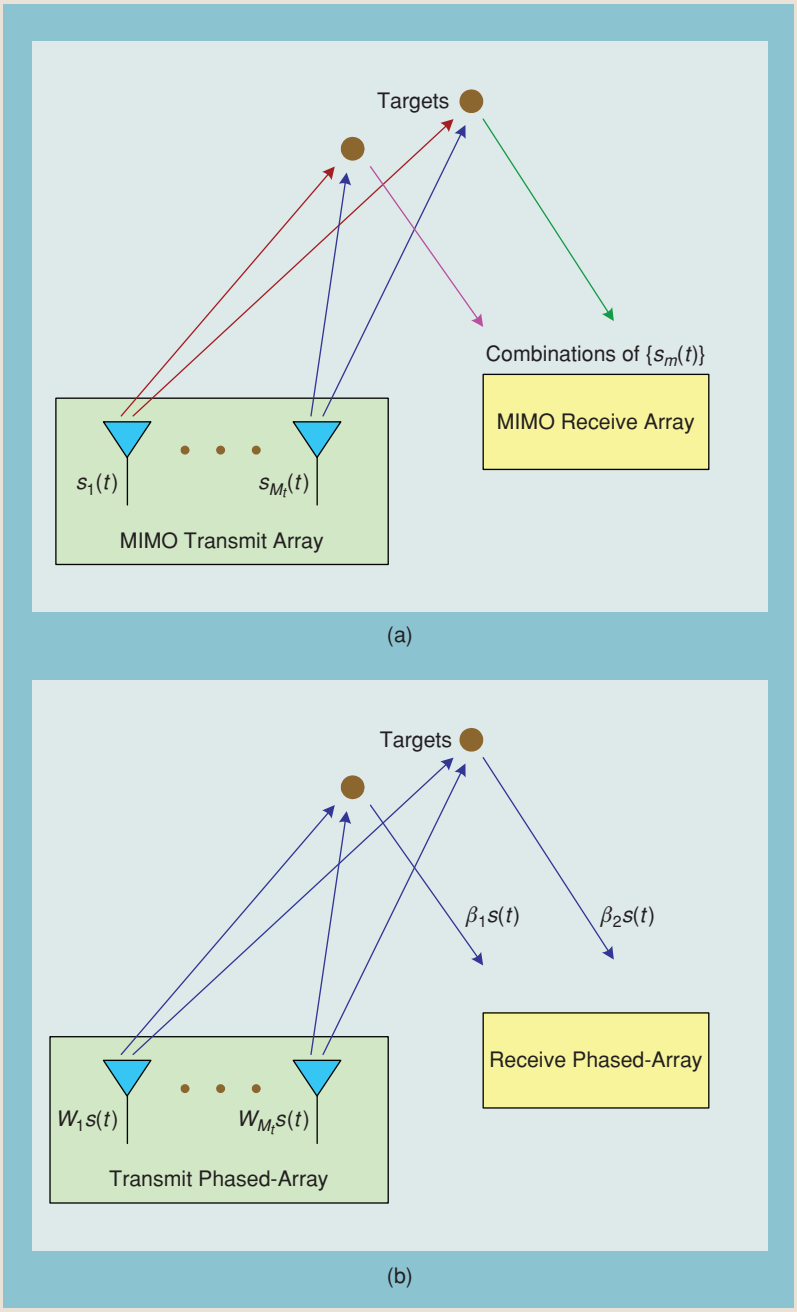

[FIG1] (a) MIMO radar versus (b) phased-array radar.

We then consider an adaptive MIMO radar scheme that can be used to deal with multiple targets. Linearly independent waveforms can be transmitted simultaneously via the multiple transmit antennas of a MIMO radar. Due to the different phase shifts associated with the different propagation paths from the transmitting antennas to targets, these independent waveforms are linearly combined at the targets with different phase factors. As a result, the signal waveforms reflected from different targets are linearly independent of each other, which allows for the direct application of Capon and of other adaptive array algorithms. We consider herein applying the Capon algorithm to estimate the target locations and an approximate maximum likelihood (AML) method recently introduced in [22] to determine the reflected signal amplitudes.

Finally, we show that the probing signal vector transmitted by a MIMO radar system can be designed to approximate a desired transmit beampattern and also to minimize the cross-correlation of the signals bounced from various targets of interest—an operation that hardly would be possible for a phased-array radar. An efficient semidefinite quadratic programming (SQP) algorithm can be used to solve the signal design problem in polynomial time. Using this design, we can significantly improve the parameter estimation accuracy of the adaptive MIMO radar techniques. In addition, we consider a minimum sidelobe beampattern design. We demonstrate the advantages of these MIMO transmit beampattern designs over their phased-array counterparts. Due to the significantly larger number of degrees of freedom (DoF) of a MIMO system, we can achieve much better transmit beampatterns with a MIMO radar, under the practical uniform elemental transmit power constraint, than with its phased-array counterpart.

PROBLEM FORMULATION

Consider a MIMO radar system with M_t transmit antennas and M_r receive antennas. Let $x_m(n)$ denote the discrete-time baseband signal transmitted by the mth transmit antenna. Also, let θ denote the location parameter(s) of a generic target, for example, its azimuth angle and its range. Then, under the assumption that the transmitted probing signals are narrowband and that the propagation is nondispersive, the baseband signal at the target location can be described by the expression (see, e.g., [7], [15] and [23], Chapter 6)

$$\sum_{m=1}^{M_t} e^{-j2\pi f_0 \tau_m(\theta)} x_m(n) \triangleq \mathbf{a}^*(\theta)\mathbf{x}(n), \quad n = 1, \cdots, N, \quad (1)$$

where f_0 is the carrier frequency of the radar, $\tau_m(\theta)$ is the time needed by the signal emitted via the m th transmit antenna to arrive at the target, $(\cdot)^*$ denotes the conjugate transpose, N denotes the number of samples of each transmitted signal pulse,

$$\mathbf{x}(n) = [x_1(n) \quad x_2(n) \quad \cdots \quad x_{M_t}(n)]^T, \quad (2)$$

and

$$\mathbf{a}(\theta) = [e^{j2\pi f_0 \tau_1(\theta)} \quad e^{j2\pi f_0 \tau_2(\theta)} \quad \cdots \quad e^{j2\pi f_0 \tau_{M_t}(\theta)}]^T, \quad (3)$$

with $(\cdot)^T$ denoting the transpose. By assuming that the transmit array of the radar is calibrated, $\mathbf{a}(\theta)$ is a known function of θ.

Let $y_m(n)$ denote the signal received by the mth receive antenna; let

$$\mathbf{y}(n) = [y_1(n) \quad y_2(n) \quad \cdots \quad y_{M_r}(n)]^T, \quad n = 1, \cdots, N, \quad (4)$$

and

$$\mathbf{b}(\theta) = [e^{j2\pi f_0 \tilde{\tau}_1(\theta)} \quad e^{j2\pi f_0 \tilde{\tau}_2(\theta)} \quad \cdots \quad e^{j2\pi f_0 \tilde{\tau}_{M_r}(\theta)}]^T, \quad (5)$$

where $\tilde{\tau}_m(\theta)$ is the time needed by the signal reflected by the target located at θ to arrive at the mth receive antenna. Then, under the simplifying assumption of point targets, the received data vector can be described by the equation (see, e.g., [3] and [14])

$$\mathbf{y}(n) = \sum_{k=1}^{K} \beta_k \mathbf{b}^c(\theta_k)\mathbf{a}^*(\theta_k)\mathbf{x}(n) + \epsilon(n), \quad n = 1, \cdots, N, \quad (6)$$

where K is the number of targets that reflect the signals back to the radar receiver, $\{\beta_k\}$ are the complex amplitudes proportional to the radar cross sections (RCSs) of those targets, $\{\theta_k\}$ are their location parameters, $\epsilon(n)$ denotes the interference-plus-noise term, and $(\cdot)^c$ denotes the complex conjugate. The unknown parameters, to be estimated from $\{\mathbf{y}(n)\}_{n=1}^N$, are $\{\beta_k\}_{k=1}^K$ and $\{\theta_k\}_{k=1}^K$.

PARAMETER IDENTIFIABILITY

Parameter identifiability is basically a consistency aspect; we want to establish the uniqueness of the solution to the parameter estimation problem as either the signal-to-interference-plus-noise ratio (SINR) goes to infinity or the snapshot number N goes to infinity [19]. It is clear that in either case, assuming that the interference-plus-noise term $\epsilon(n)$ is uncorrelated with $\mathbf{x}(n)$, the identifiability property of the first term in (6) is not affected by the second term. In particular, it follows that asymptotically, we can handle any number of interferences. Of course, for a finite snapshot number N and a finite SINR, the accuracy will degrade as the number of interferences increases, but that is a different issue—the parameter identifiability is not affected.

Using results from [24] and [25], we can show that when the M_t transmitted waveforms are linearly independent of each other, a sufficient and generically (for almost every vector β) necessary condition for parameter identifiability is

$$K_{\max} \in \left[\frac{M_t + M_r - 2}{2}, \frac{M_t M_r + 1}{2}\right), \quad (7)$$

depending on the array geometry and how many antennas are shared between the transmit and receive arrays [19].

Furthermore, generically, (i.e., for almost any vector β), the identifiability can be ensured under the following condition [19], [24]:

$$K_{\max} \in \left[\frac{2(M_t + M_r) - 5}{3}, \frac{2M_t M_r}{3} \right), \tag{8}$$

which typically yields a larger number $K_{\max}$ than the one given in (7).

For a phased-array radar, the condition similar to (7) is

$$K_{\max} = \left\lceil \frac{M_r - 1}{2} \right\rceil, \tag{9}$$

and that similar to (8) is

$$K_{\max} = \left\lceil \frac{2M_r - 3}{3} \right\rceil, \tag{10}$$

where $\lceil \cdot \rceil$ denotes the smallest integer greater than or equal to a given number.

Hence, the maximum number of targets that can be uniquely identified by a MIMO radar can be up to M_t times that of its phased-array counterpart. To illustrate the extreme cases, note that when a filled (i.e., 0.5-wavelength interelement spacing) uniform linear array (ULA) is used for both transmitting and receiving, which appears to be the worst MIMO radar scenario from the parameter identifiability standpoint, the maximum number of targets that can be identified by the MIMO radar is about twice that of its phased-array counterpart. This is because the virtual aperture $\mathbf{b}^c(\theta) \otimes \mathbf{a}^c(\theta)$ of the MIMO radar system has only $M_t + M_r - 1$ distinct elements. On the other hand, when the receive array is a filled ULA with M_r elements and the transmit array is a sparse ULA comprising M_t elements with $M_r/2$-wavelength interelement spacing, the virtual aperture of the MIMO radar system is a filled-element ($M_t M_r$) ULA, i.e., the virtual aperture length is M_t times that of the receive array [4], [19]. This increased virtual aperture size for this case leads to the result that the maximum number of targets that can be uniquely identified by the MIMO radar is M_t times that of its phased-array counterpart.

We present several numerical examples to demonstrate the parameter identifiability of MIMO radar, as compared to its phased-array counterpart. First, consider a MIMO radar system where a ULA with $M = M_t = M_r = 10$ antennas and half-wavelength spacing between adjacent antennas is used both for transmitting and receiving. The transmitted waveforms are orthogonal to each other. Consider a scenario in which K targets are located at $\theta_1 = 0^\circ$, $\theta_2 = 10^\circ$, $\theta_3 = -10^\circ$, $\theta_4 = 20^\circ$, $\theta_5 = -20^\circ$, $\theta_6 = 30^\circ$, $\theta_7 = -30^\circ$, $\cdots$, with identical complex amplitudes $\beta_1 = \cdots = \beta_K = 1$. The number of snapshots is $N = 256$. The received signal is corrupted by a spatially and temporally white circularly symmetric complex Gaussian noise with mean zero and variance 0.01 [i.e., signal-to-noise ratio (SNR) = 20 dB] and by a jammer located at 45° with an unknown waveform (uncorrelated with the waveforms transmitted by the radar) with a variance equal to 1 [i.e., interference-to-noise ratio (INR) = 20 dB].

Consider the CRB of $\{\theta_k\}$, which gives the best performance of an unbiased estimator. By assuming that $\{\epsilon(n)\}_{n=1}^N$ in (6) are independently and identically distributed (i.i.d.) circularly symmetric complex Gaussian random vectors with mean zero and unknown covariance $\mathbf{Q}$, the CRB for $\{\theta_k\}$ can be obtained using the Slepian-Bangs formula [23]. Figure 2(a) shows the CRB of θ_1 for the MIMO radar as a function of K. For comparison purposes, we also provide the CRB of its phased-array counterpart, for which all the parameters are the same as for the MIMO radar except that $M_t = 1$ and that the amplitude of the transmitted waveform is adjusted so that the total transmission power does not change. Note that the phased-array CRB increases rapidly as K increases from 1 to 6. The corresponding MIMO CRB, however, is almost constant when K is varied from 1 to 12 (but becomes unbounded for $K > 12$). Both results are consistent with the parameter identifiability analysis (see [19] for details): $K_{\max} \leq 6$ for the phased-array radar and $K_{\max} \leq 12$ for the MIMO radar.

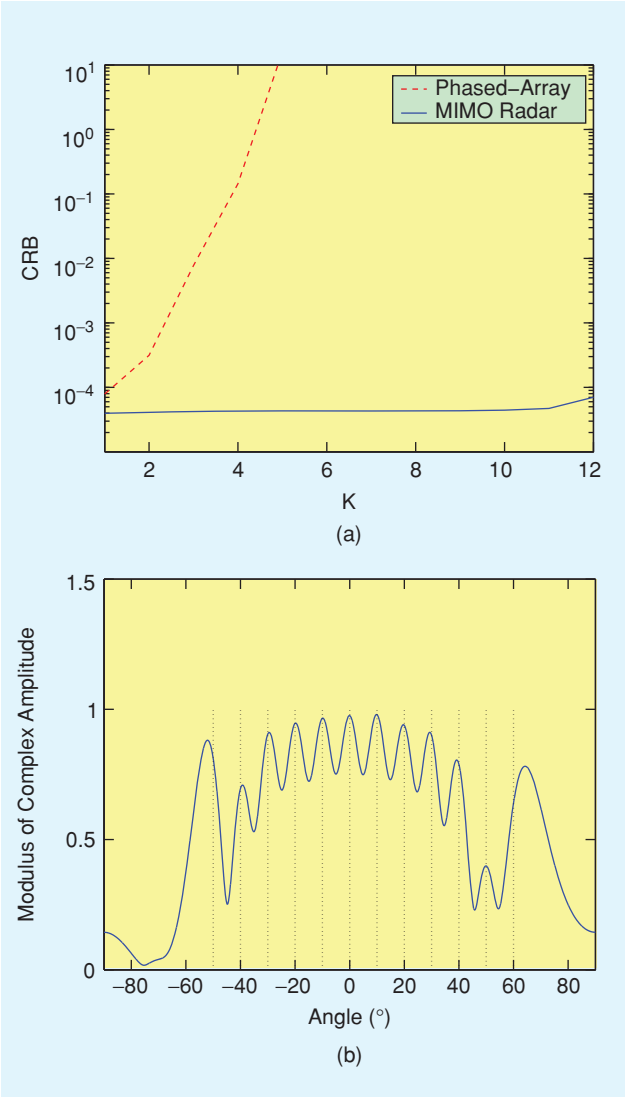

[FIG2] Performance of a MIMO radar system where a ULA with $M = 10$ antennas and 0.5-wavelength interelement spacing is used for both transmitting and receiving. (a) CRB of θ_1 versus K and (b) LS spatial spectrum when $K = 12$.

We next consider a simple semiparametric least-squares (LS) method [14] for MIMO radar parameter estimation. Figure 2(b) shows the LS spatial spectrum as a function θ, when $K = 12$. Note that all 12 target locations can be approximately determined from the peak locations of the LS spatial spectrum.

A MULTI-INPUT MULTI-OUTPUT RADAR SYSTEM CAN TRANSMIT MULTIPLE PROBING SIGNALS THAT MAY BE CORRELATED OR UNCORRELATED WITH EACH OTHER.

Consider now a MIMO radar system with $M_t = M_r = 5$ antennas. The distance between adjacent antennas is 0.5-wavelength for the receiving ULA and 2.5-wavelength for the transmitting ULA. We retain all the simulation parameters corresponding to Figure 2 except that the targets are located at $\theta_1 = 0^\circ$, $\theta_2 = 8^\circ$, $\theta_3 = -8^\circ$, $\theta_4 = 16^\circ$, $\theta_5 = -16^\circ$, $\theta_6 = 24^\circ$, $\theta_7 = -24^\circ$, $\cdots$ in this example. Figure 3(a) shows the CRB of θ_1, for both the MIMO radar and the phased-array counterpart, as a function of K. Again, the MIMO CRB is much lower than the phased-array CRB. The behavior of both CRBs is consistent with the parameter identifiability analysis: $K_{\max} \leq 3$ for the phased-array radar and $K_{\max} \leq 16$ for the MIMO radar. Moreover, the parameters of all $K = 16$ targets can be approximately determined with the simple LS method, as shown in Figure 3(b).

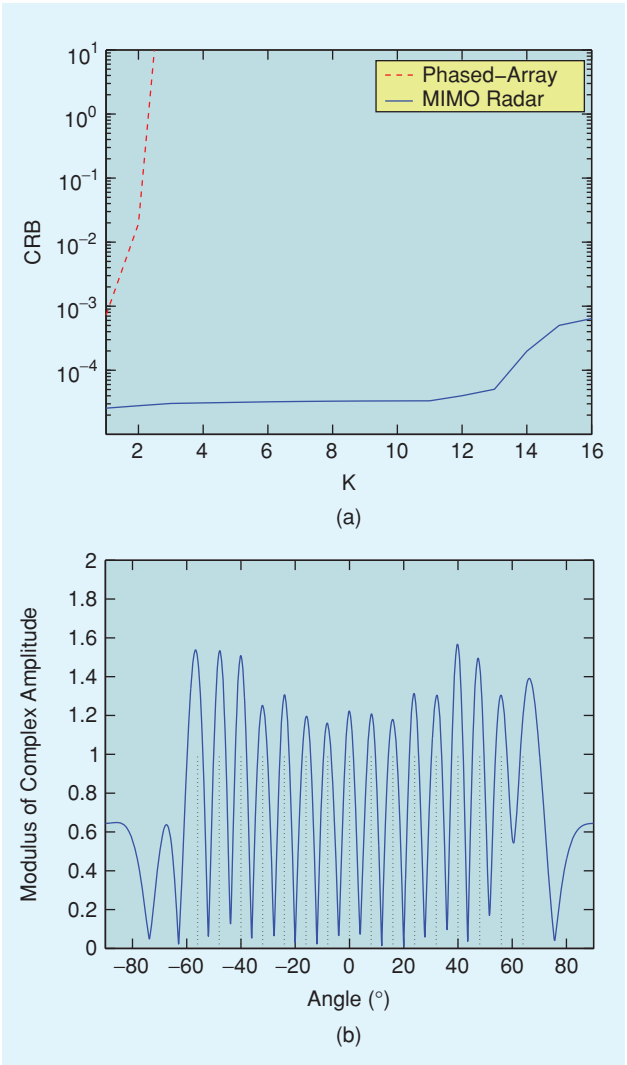

[FIG3] Performance of a MIMO radar system with $M_t = M_r = 5$ antennas, and with half-wavelength interelement spacing for the receive ULA and 2.5-wavelength interelement spacing for the transmit ULA. (a) CRB of θ_1 versus K and (b) LS spatial spectrum when $K = 16$.

DIRECT APPLICATION OF ADAPTIVE TECHNIQUES FOR PARAMETER ESTIMATION

As shown recently in [14], MIMO radar makes it possible to use adaptive localization and detection techniques directly, unlike a phased-array radar. This is another significant advantage of a MIMO radar system since adaptive techniques are known to have much better resolution and much better interference rejection capability than their data-independent counterparts. For example, in space-time adaptive processing applications, secondary range bins are needed to be able to use adaptive techniques [26]–[28]; however, selecting quality secondary range bins is in itself a major challenge [29]. Since the MIMO probing signals reflected back by the targets are actually linearly independent of each other, the direct application of adaptive techniques is made possible for a MIMO radar system without the need for secondary range bins or even for range compression [20].

Let

$$\tilde{\mathbf{A}} = [\beta_1^* \mathbf{a}(\theta_1) \quad \beta_2^* \mathbf{a}(\theta_2) \quad \cdots \quad \beta_K^* \mathbf{a}(\theta_K)]. \tag{11}$$

Then the sample covariance matrix of the target reflected waveforms is $\tilde{\mathbf{A}}^* \hat{\mathbf{R}}_{xx} \tilde{\mathbf{A}}$, where $\hat{\mathbf{R}}_{xx} = (1/N) \sum_{n=1}^{N} \mathbf{x}(n)\mathbf{x}^*(n)$. For example, when orthogonal waveforms are used for MIMO probing and $N \geq M_t$, $\hat{\mathbf{R}}_{xx}$ is a scaled identity matrix. Then $\tilde{\mathbf{A}}^* \hat{\mathbf{R}}_{xx} \tilde{\mathbf{A}}$ has full rank, i.e., the target reflected waveforms are not completely correlated with each other (or coherent), if the columns of $\tilde{\mathbf{A}}$ are linearly independent of each other, which requires that $K \leq M_t$. The fact that the target reflected waveforms are noncoherent allows the direct application of many adaptive techniques for target localization [14].

We demonstrate the performance of the Capon method for target localization. Consider the scenario of a MIMO radar with a ULA comprising $M = M_t = M_r = 10$ antennas with half-wavelength spacing between adjacent antennas. This array is used both for transmitting and receiving. Without loss of generality, the total transmit power is set to 1. Assume that $K = 3$ targets are located at $\theta_1 = -40^\circ$, $\theta_2 = 0^\circ$, and $\theta_3 = 40^\circ$ with complex amplitudes equal to $\beta_1 = \beta_2 = \beta_3 = 1$. There is a strong jammer at 25° with an unknown waveform (uncorrelated with the transmitted MIMO radar waveforms) with a power equal to 10^6 (60 dB). Each transmitted signal pulse has $N = 256$ samples. The received signal

is also corrupted by a zero-mean circularly symmetric spatially and temporally white Gaussian noise with variance σ^2.

Since we do not assume any prior knowledge about the target locations, orthogonal waveforms are used for MIMO probing. (We refer to this as initial probing, since after we get the target location estimates with this probing, we can optimize the transmitted beampattern to improve the estimation accuracy, as shown in the following section.) Using the data collected as a result of this initial probing, we can obtain the Capon spatial spectrum and the generalized likelihood ratio test (GLRT) function [14]. An example of the Capon spectrum for $\sigma^2 = -10$ dB is shown in Figure 4(a), where very narrow peaks occur around the target locations. Note that in Figure 4(a), a false peak occurs around $\theta = 25^\circ$ due to the presence of the very strong jammer. The corresponding GLRT pseudo-spectrum as a function of θ is shown in Figure 4(b). Note that the GLRT is close to one at the target locations and close to zero at any other locations including the jammer location. Therefore, the GLRT can be used to reject the jammer peak in the Capon spectrum. The remaining peak locations in the Capon spectrum are the estimated target locations.

THE MAXIMUM NUMBER OF TARGETS THAT CAN BE UNIQUELY IDENTIFIED BY A MIMO RADAR CAN BE UP TO M_t TIMES THAT OF ITS PHASED-ARRAY COUNTERPART.

PROBING SIGNAL DESIGN

The probing signal vector transmitted by a MIMO radar system can be designed to approximate a desired transmit beampattern and also to minimize the cross-correlation of the signals bounced from various targets of interest—an operation that, like the direct application of adaptive techniques, would be hardly possible for a phased-array radar [7], [15]–[17].

The power of the probing signal at a generic focal point with location θ is given by [see (1)]

$$P(\theta) = \mathbf{a}^*(\theta)\mathbf{R}\mathbf{a}(\theta), \tag{12}$$

where $\mathbf{R}$ is the covariance matrix of $\mathbf{x}(n)$, i.e.,

$$\mathbf{R} = E\{\mathbf{x}(n)\mathbf{x}^*(n)\}. \tag{13}$$

The spatial spectrum in (12), as a function of θ, will be called the transmit beampattern.

The first problem we will consider in this section consists of choosing $\mathbf{R}$ under a uniform elemental power constraint,

$$R_{mm} = \frac{c}{M}, \quad m = 1, \cdots, M; \quad \text{with } c \text{ given}, \tag{14}$$

where M is a short notation for M_t, R_{mm} denotes the (m, m)th element of $\mathbf{R}$, to achieve the following goals:

- Control the spatial power at a number of given target locations by matching (or approximating) a desired transmit beampattern.
- Minimize the cross-correlation between the probing signals at a number of given target locations; note from (1) that the cross-correlation between the probing signals at locations θ and $\bar{\theta}$ is given by $\mathbf{a}^*(\theta)\mathbf{R}\mathbf{a}(\bar{\theta})$.

Let $\phi(\theta)$ denote a desired transmit beampattern, and let $\{\mu_l\}_{l=1}^{L}$ be a fine grid of points that cover the location sectors of interest. We assume that the said grid contains points which are good approximations of the locations $\{\theta_k\}_{k=1}^{\tilde{K}}$ of the targets of interest, and that we dispose of (initial) estimates $\{\hat{\theta}_k\}_{k=1}^{\tilde{K}}$ of $\{\theta_k\}_{k=1}^{\tilde{K}}$, where $\tilde{K}$ denotes the number of targets of interest that we wish to probe further. We can obtain $\phi(\theta)$ and $\{\hat{\theta}_k\}_{k=1}^{\tilde{K}}$ using the Capon and GLRT approaches presented in the previous section.

As stated above, our goal is to choose $\mathbf{R}$ such that the transmit beampattern, $\mathbf{a}^*(\theta)\mathbf{R}\mathbf{a}(\theta)$, matches or rather approximates [in a least squares (LS) sense] the desired transmit beampattern, $\phi(\theta)$, over the sectors of interest, and also such that the cross-correlation (beam)pattern, $\mathbf{a}^*(\theta)\mathbf{R}\mathbf{a}(\bar{\theta})$ (for $\theta \neq \bar{\theta}$), is minimized (once again, in an LS sense) over the set $\{\hat{\theta}_k\}_{k=1}^{\tilde{K}}$. Mathematically, we want to solve the following problem

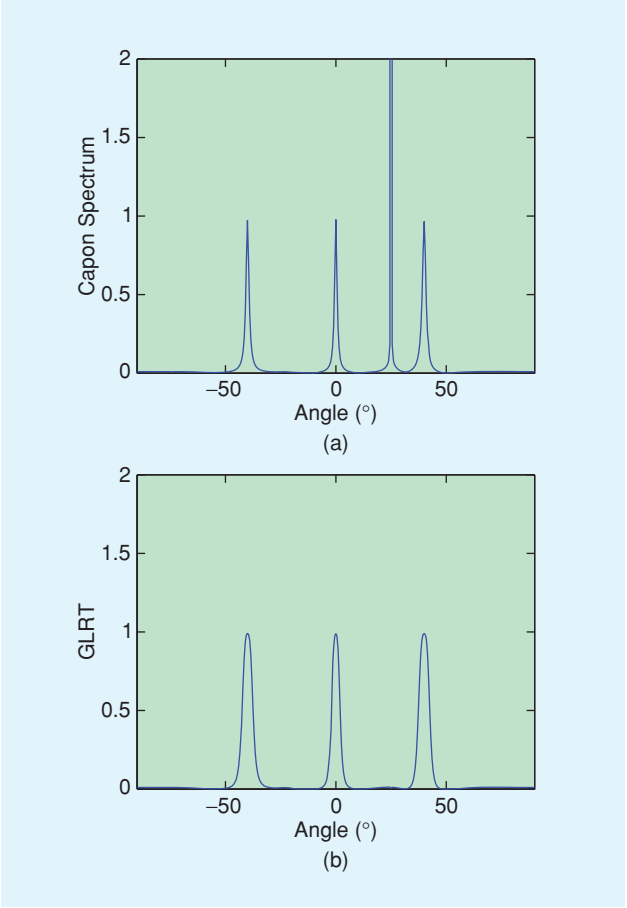

[FIG4] **(a) The Capon spatial spectrum and (b) the GLRT pseudo-spectrum as functions of θ, for the initial omnidirectional probing.**

$$\min_{\alpha,\mathbf{R}} \quad \left\{ \frac{1}{L}\sum_{l=1}^{L} w_l \left[\alpha\phi(\mu_l) - \mathbf{a}^*(\mu_l)\mathbf{R}\mathbf{a}(\mu_l)\right]^2 + \frac{2w_c}{\tilde{K}^2-\tilde{K}} \sum_{k=1}^{\tilde{K}-1}\sum_{p=k+1}^{\tilde{K}} \left|\mathbf{a}^*(\hat{\theta}_k)\mathbf{R}\mathbf{a}(\hat{\theta}_p)\right|^2 \right\}$$
$$\text{s.t.} \quad R_{mm} = \frac{c}{M}, \quad m = 1, \cdots, M$$
$$\mathbf{R} \geq 0, \tag{15}$$

where α is a scaling factor, $w_l \geq 0$, $l = 1, \cdots, L$, is the weight for the lth grid point and $w_c \geq 0$ is the weight for the cross-correlation term. The reason for introducing α in the design problem is that typically $\phi(\theta)$ is given in a normalized form (e.g., satisfying $\phi(\theta) \leq 1, \forall\theta$), and our interest lies in approximating an appropriately scaled version of $\phi(\theta)$, not $\phi(\theta)$ itself. The value of w_l should be larger than that of w_k if the beampattern matching at μ_l is considered to be more important than the matching at μ_k. Note that by choosing $\max_l w_l > w_c$ we can give more weight to the first term in the design criterion above, and viceversa for $\max_l w_l < w_c$. We show in [15], [17] that this design problem can be efficiently solved in polynomial time as a SQP.

To illustrate the beampattern matching design, consider the example considered in Figure 4. The initial target location estimates obtained using Capon or GLRT can be used to derive a desired beampattern. In the following numerical examples, we form the desired beampattern by using the dominant peak locations of the GLRT pseudo-spectrum, denoted as $\hat{\theta}_1, \cdots, \hat{\theta}_{\hat{K}}$, as follows (with $\hat{K}$ being the resulting estimate of K, and $\tilde{K} = \hat{K}$):

$$\phi(\theta) = \begin{cases} 1, & \theta \in [\hat{\theta}_k - \Delta, \hat{\theta}_k + \Delta], \quad k = 1, \cdots, \hat{K}, \\ 0, & \text{otherwise}, \end{cases} \tag{16}$$

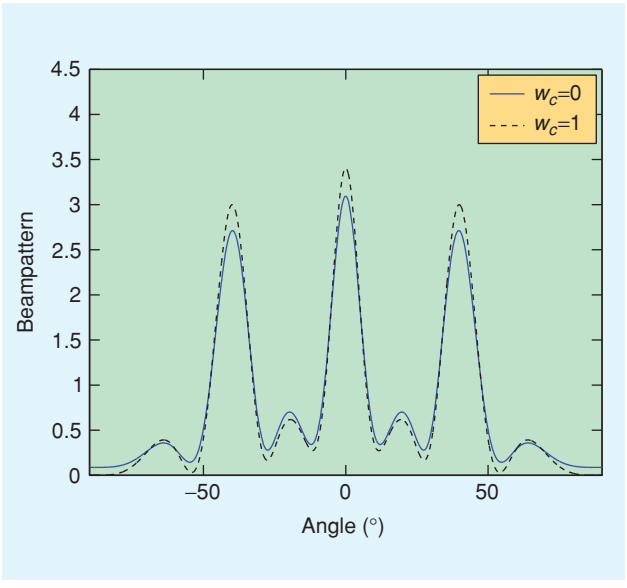

[FIG5] MIMO beampattern matching designs for $\Delta = 5^\circ$ and $c = 1$. The beampatterns are obtained using $w_c = 0$ or $w_c = 1$.

where 2Δ is the chosen beamwidth for each target (Δ should be greater than the expected error in $\{\hat{\theta}_k\}$). Figure 5 is obtained using (16) with $\Delta = 5^\circ$ in the beampattern matching design in (15) along with a mesh grid size of 0.1°, $w_l = 1$, $l = 1, \cdots, L$, and either $w_c = 0$ or $w_c = 1$. Note that the designs obtained with $w_c = 1$ and with $w_c = 0$ are similar to one another. However, the cross-correlation behavior of the former is much better than that of the latter in that the reflected signal waveforms corresponding to using $w_c = 1$ are almost uncorrelated with each other.

Next, we examine the mean-squared errors (MSEs) of the location estimates obtained by Capon and of the complex amplitude estimates obtained by AML [22]. In particular, we compare the MSEs obtained using the initial omnidirectional probing with those obtained using the optimal beampattern matching design shown in Figure 5 with $\Delta = 5^\circ$ and

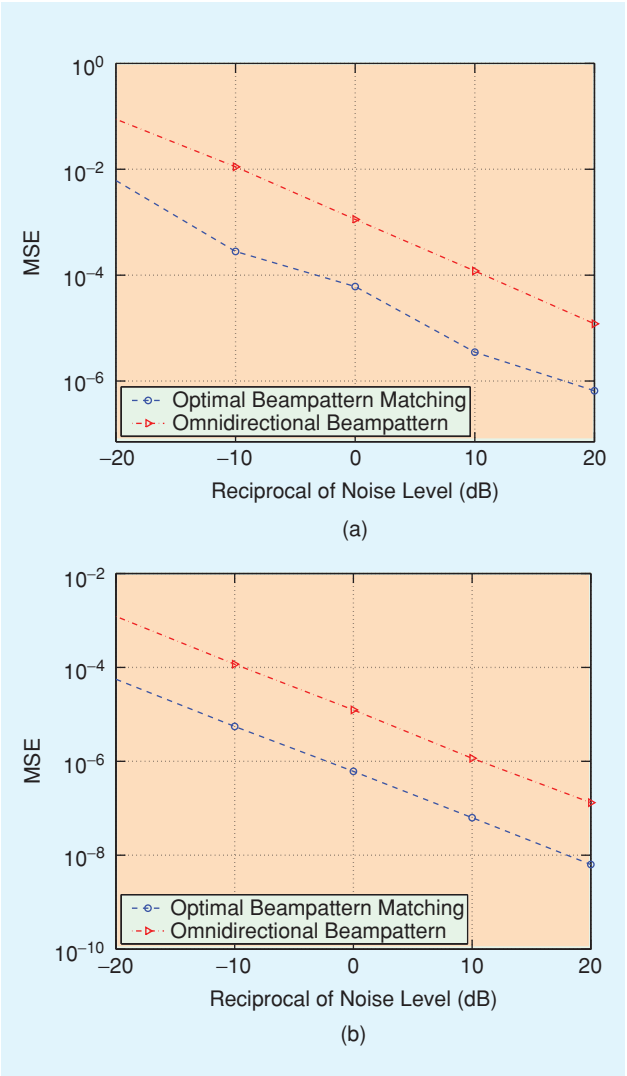

[FIG6] MSEs of (a) the location estimates and (b) the complex amplitude estimates for the first target as functions of $-10\log_{10}\sigma^2$, obtained with initial omnidirectional probing and probing using the beampattern matching design for $\Delta = 5^\circ$, $w_c = 1$, and $c = 1$.

$w_c = 1$. Figure 6(a) and (b) shows the MSE curves of the location and complex amplitude estimates obtained for the target at -40° from 1,000 Monte-Carlo trials (the results for the other targets are similar). The estimates obtained using the optimal beampattern matching design are much better: the SNR gain over the omnidirectional design is larger than 10 dB.

Another beampattern design problem we consider consists of choosing $\mathbf{R}$ under the uniform elemental power constraint in (14) to achieve the following goals:

- Minimize the sidelobe level in a prescribed region.
- Achieve a predetermined 3 dB main-beam width.

This problem can be formulated as follows:

$$\begin{aligned} \min_{t,\mathbf{R}} \quad & -t \\ \text{s.t.} \quad & \mathbf{a}^*(\theta_0)\mathbf{R}\mathbf{a}(\theta_0) - \mathbf{a}^*(\mu_l)\mathbf{R}\mathbf{a}(\mu_l) \geq t, \quad \forall\, \mu_l \in \Omega \\ & \mathbf{a}^*(\theta_1)\mathbf{R}\mathbf{a}(\theta_1) = 0.5\mathbf{a}^*(\theta_0)\mathbf{R}\mathbf{a}(\theta_0) \\ & \mathbf{a}^*(\theta_2)\mathbf{R}\mathbf{a}(\theta_2) = 0.5\mathbf{a}^*(\theta_0)\mathbf{R}\mathbf{a}(\theta_0) \\ & \mathbf{R} \geq 0 \\ & R_{mm} = \frac{c}{M}, \quad m = 1, \cdots, M, \end{aligned} \tag{17}$$

where $\theta_2 - \theta_1$ (with $\theta_2 > \theta_0$ and $\theta_1 < \theta_0$) determines the 3 dB main-beam width and Ω denotes the sidelobe region of interest. As shown in [15] and [17], this minimum sidelobe beampattern design problem can be efficiently solved in polynomial time as a semidefinite program (SDP).

Finally, consider the conventional phased-array beampattern design problem in which only the array weight vector can be adjusted and therefore all antennas transmit the same differently scaled waveform. We can readily modify the previously described beampattern matching or minimum sidelobe beampattern designs for the case of phased-arrays by adding the constraint $\text{rank}(\mathbf{R}) = 1$. However, due to the rank-one constraint, both these originally convex optimization problems become non-convex. The lack of convexity makes the rank-one constrained problems much harder to solve than the original convex optimization problems [30]. Semidefinite relaxation (SDR) is often used to obtain approximate solutions to such rank-constrained optimization problems [31]. Typically, the SDR is obtained by omitting the rank constraint. Hence, interestingly, the MIMO beampattern design problems are SDRs of the corresponding phased-array beampattern design problems.

In the numerical examples below, we have used the Newton-like algorithm presented in [30] to solve the rank-one constrained design problems for phased-arrays. This algorithm uses SDR to obtain an initial solution, which is the exact solution to the corresponding MIMO beampattern design problem. Although the convergence of the said Newton-like algorithm is not guaranteed [30], we did not encounter any apparent problem in our numerical simulations.

MIMO RADAR MAKES IT POSSIBLE TO USE ADAPTIVE LOCALIZATION AND DETECTION TECHNIQUES DIRECTLY.

Consider the minimum sidelobe beampattern design problem in (17), with the main beam centered at $\theta_0 = 0^\circ$, with a 3 dB width equal to 20° ($\theta_2 = -\theta_1 = 10^\circ$), and with $c = 1$, for the same MIMO radar scenario as the one considered in Figure 4. The sidelobe region is $\Omega = [-90^\circ, -20^\circ] \cup [20^\circ, 90^\circ]$. The MIMO minimum-sidelobe beampattern design is shown in Figure 7(a). Note that the peak sidelobe level achieved by the MIMO design is approximately 18 dB below the mainlobe peak level. Figure 7(b) shows the corresponding phased-array beampattern obtained by using the additional constraint $\text{rank}(\mathbf{R}) = 1$. The phased-array design fails to provide a proper mainlobe (it suffers from peak splitting) and its peak sidelobe level is much higher than that of its MIMO counterpart. We note

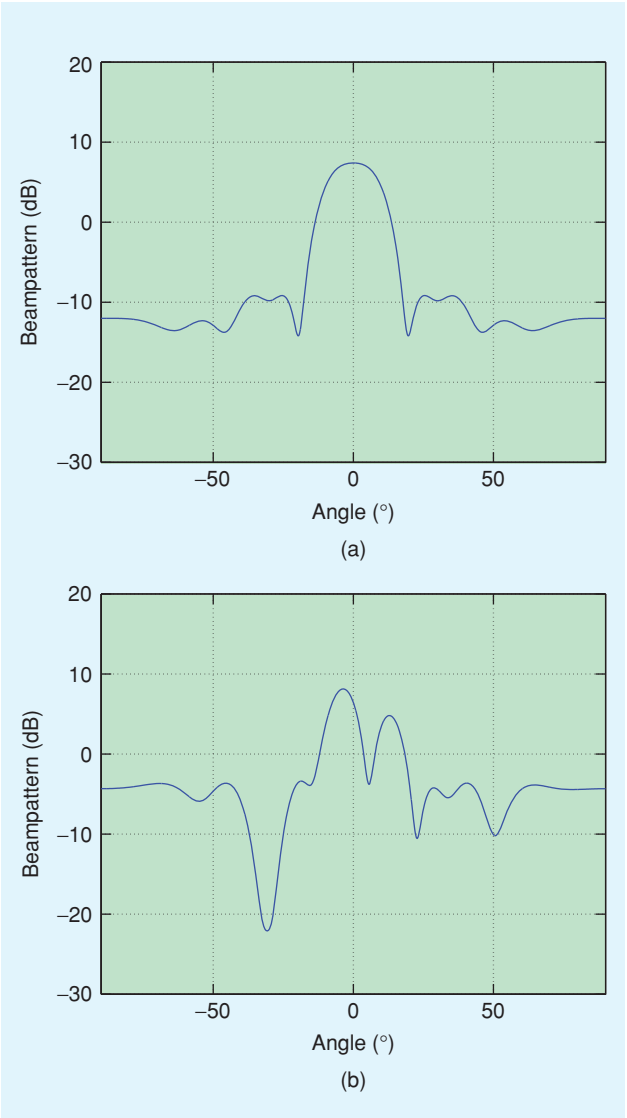

[FIG7] Minimum sidelobe beampattern designs under the uniform elemental power constraint when the 3 dB main beam width is 20°. (a) MIMO and (b) phased-array.

that, under the elemental power constraint, the number of DoF of the phased-array that can be used for beampattern design is equal to only $M-1$ (real-valued parameters); consequently, it is difficult for the phased-array to synthesize a proper beampattern. The MIMO design, on the other hand, can be used to achieve a much better beampattern due to its much larger number of DoF, i.e., M^2-M.

CONCLUSIONS

We have provided a review of some recent results on the emerging technology of MIMO radar with colocated antennas. We have shown that the waveform diversity offered by such a MIMO radar system enables significant superiority over its phased-array counterpart, including much improved parameter identifiability, direct applicability of adaptive techniques for parameter estimation, as well as superior flexibility of transmit beampattern designs. We hope that this overview of our recent results on the MIMO radar, along with the related results obtained by our colleagues, will stimulate the interest deserved by this topic in both academia and government agencies as well as industry.

ACKNOWLEDGMENT

This work was supported in part by the National Science Foundation under Grant No. CCF-0634786 and the Swedish Research Council (VR). Opinions, interpretations, conclusions, and recommendations are those of the authors and are not necessarily endorsed by the United States Government.

AUTHORS

Jian Li (li@dsp.ufl.edu) received the M.Sc. and Ph.D. degrees in electrical engineering from The Ohio State University, Columbus in 1987 and 1991, respectively. She is a professor with the Department of Electrical and Computer Engineering, University of Florida, Gainesville. Her current research interests include spectral estimation, statistical and array signal processing, and their applications. She is a Fellow of IEEE and IET. She is presently a member of two of the IEEE Signal Processing Society technical committees: Signal Processing Theory and Methods (SPTM) Technical Committee and Sensor Array and Multichannel (SAM) Technical Committee.

Petre Stoica is a professor of system modeling at Uppsala University, Uppsala, Sweden. Additional information is available at http://user.it.uu.se/ps/ps.html.

REFERENCES

[1] E. Fishler, A. Haimovich, R. Blum, D. Chizhik, L. Cimini, and R. Valenzuela, "MIMO radar: An idea whose time has come," in *Proc. IEEE Radar Conf.*, Apr. 2004, pp. 71–78.

[2] E. Fishler, A. Haimovich, R. Blum, L. Cimini, D. Chizhik, and R. Valenzuela, "Performance of MIMO radar systems: Advantages of angular diversity," in *Proc. 38th Asilomar Conf. Signals, Syst. Comput.*, Pacific Grove, CA, Nov. 2004, vol. 1, pp. 305–309.

[3] E. Fishler, A. Haimovich, R. Blum, L. Cimini, D. Chizhik, and R. Valenzuela, "Spatial diversity in radars—models and detection performance," *IEEE Trans. Signal Processing*, vol. 54, Mar. 2006, pp. 823–838.

[4] D.W. Bliss and K.W. Forsythe, "Multiple-input multiple-output (MIMO) radar and imaging: Degrees of freedom and resolution," in *Proc. 37th Asilomar Conf. Signals, Syst. Comput.*, Pacific Grove, CA, Nov. 2003, vol. 1, pp. 54–59.

[5] I. Bekkerman and J. Tabrikian, "Spatially coded signal model for active arrays," in *Proc. 2004 IEEE Int. Conf. Acoustics, Speech, and Signal Processing*, Montreal, Quebec, Canada, Mar. 2004, vol. 2, pp. ii/209–ii/212.

[6] K. Forsythe, D. Bliss, and G. Fawcett, "Multiple-input multiple-output (MIMO) radar: Performance issues," in *Proc. 38th Asilomar Conf. Signals, Syst. Comput.*, Pacific Grove, CA, Nov. 2004, vol. 1, pp. 310–315.

[7] D.R. Fuhrmann and G. San Antonio, "Transmit beamforming for MIMO radar systems using partial signal correlations," in *Proc. 38th Asilomar Conf. Signals, Syst. Comput.*, Pacific Grove, CA, Nov. 2004, vol. 1, pp. 295–299.

[8] F.C. Robey, S. Coutts, D. Weikle, J.C. McHarg, and K. Cuomo, "MIMO radar theory and exprimental results," in *Proc. 38th Asilomar Conf. Signals, Syst. Comput.*, Pacific Grove, CA, Nov. 2004, vol. 1, pp. 300–304.

[9] J. Tabrikian and I. Bekkerman, "Transmission diversity smoothing for multi-target localization," in *Proc. 2005 IEEE Int. Conf. Acoustics, Speech, and Signal Processing*, Philadelphia, PA, Mar. 2005, vol. 4, pp. iv/1041–iv/1044.

[10] K.W. Forsythe and D.W. Bliss, "Waveform correlation and optimization issues for MIMO radar," in *Proc. 39th Asilomar Conf. Signals, Syst. Comput.*, Pacific Grove, CA, Nov. 2005, pp. 1306–1310.

[11] J. Li and P. Stoica, "MIMO radar—diversity means superiority," in *Proc. 14th Annu. Workshop Adaptive Sensor Array Processing*, MIT Lincoln Laboratory, Lexington, MA, June 2006.

[12] J. Tabrikian, "Barankin bounds for target localization by MIMO radars," in *Proc. 4th IEEE Workshop on Sensor Array and Multi-Channel Processing*, Waltham, MA, pp. 278–281, July 2006.

[13] L. Xu, J. Li, and P. Stoica, "Adaptive techniques for MIMO radar," in *Proc. 4th IEEE Workshop on Sensor Array and Multi-Channel Processing*, Waltham, MA, pp. 258–262, July 2006.

[14] L. Xu, J. Li, and P. Stoica, "Radar imaging via adaptive MIMO techniques," in *Proc. 14th European Signal Processing Conf.*, Florence, Italy, Sept. 2006.

[15] J. Li, P. Stoica, and Y. Xie, "On probing signal design for MIMO radar," in *Proc. 40th Asilomar Conf. Signals, Syst. Comput.* (invited), Pacific Grove, CA, pp. 31–35, Oct. 2006.

[16] D.R. Fuhrmann and G. San Antonio, "Transmit beamforming for MIMO radar systems using signal cross-correlation," *IEEE Trans. Aerosp. Electron. Syst.* To be published.

[17] P. Stoica, J. Li, and Y. Xie, "On probing signal design for MIMO radar," *IEEE Trans. Signal Processing.* To be published.

[18] I. Bekkerman and J. Tabrikian, "Space-time coding for active arrays," *IEEE Trans. Signal Processing*, 2006. To be published.

[19] J. Li, P. Stoica, L. Xu, and W. Roberts, "On parameter identifiability of MIMO radar," *IEEE Signal Processing Lett.* To be published.

[20] L. Xu, J. Li, P. Stoica, K.W. Forsythe, and D.W. Bliss, "Waveform optimization for MIMO radar: A Cramer-Rao bound based study," in *Proc. 2007 IEEE Int. Conf. Acoustics, Speech, and Signal Processing*, Honolulu, Hawaii, pp. II-917–11-920, Apr. 2007.

[21] J. Li, L. Xu, P. Stoica, K. Forsythe, and D. Bliss, "Range compression and waveform optimization for MIMO radar: A Cramér-Rao bound based study," *IEEE Trans. Signal Processing*, 2006.

[22] L. Xu, P. Stoica, and J. Li, "A diagonal growth curve model and some signal processing applications," *IEEE Trans. Signal Processing*, vol. 54, pp. 3363–3371, Sept. 2006.

[23] P. Stoica and R.L. Moses, *Spectral Analysis of Signals*. Upper Saddle River, NJ: Prentice-Hall, 2005.

[24] M. Wax and I. Ziskind, "On unique localization of multiple sources by passive sensor arrays," *IEEE Trans. Acoustics, Speech, and Signal Processing*, vol. 37, issue 7, pp. 996–1000, July 1989.

[25] A. Nehorai, D. Starer, and P. Stoica, "Direction-of-arrival estimation in applications with multipath and few snapshots," *Circuits, Syst. Signal Process.*, vol. 10, issue 3, pp. 327–342, 1991.

[26] J. Ward, "Space-time adaptive processing for airborne radar," MIT Lincoln Laboratory, Lexington, MA, Tech. Rep. 1015, Dec. 1994.

[27] R. Klemm, *Principles of Space-Time Adaptive Processing*. London, U.K.: IEE Press, 2002.

[28] J.R. Guerci, *Space-Time Adaptive Processing for Radar*. Norwood, MA: Artech House, 2003.

[29] D.J. Rabideau and A.O. Steinhardt, "Improved adaptive clutter cancellation through data-adaptive training," *IEEE Trans. Aerosp. Electron. Syst.*, vol. 35, pp. 879–891, July 1999.

[30] R. Orsi, U. Helmke, and J.B. Moore, "A Newton-like method for solving rank constrained linear matrix inequalities," in *Proc. 43rd IEEE Conf. Decision and Control*, 2004, pp. 3138–3144.

[31] S. Boyd and L. Vandenberghe, *Convex Optimization*. Cambridge, U.K.: Cambridge Univ. Press, 2004. SP